Journal of Applied Electrochemistry **30**: 117–120, 2000.

Short communication

Electrodeposition studies in the MnO_2 + PbO_2 system: formation of $Pb_3Mn_7O_{15}$

E.A. DALCHIELE[1], S. CATTARIN[2], M. MUSIANI[2], U. CASELLATO[3] and P. GUERRIERO[3]
[1]*Instituto de Física, Herrera y Reissig 565, C.C. 30, 11000 Montevideo, Uruguay;*
[2]*IPELP CNR Corso Stati Uniti 4, 35127 Padova, Italy;*
[3]*ICTIMA CNR Corso Stati Uniti 4, 35127 Padova, Italy*

Received 18 January 1999; accepted in revised form 6 July 1999

Key words: annealing, anodic deposition, metal oxides, mixed oxides, $Pb_3Mn_7O_{15}$

1. Introduction

Metal oxides are the object of continuous research due to their importance in many electrochemical applications like batteries [1] and electrocatalysis [2]. As well as pure oxides, many mixed oxides have been obtained and characterised. For instance PbO_2 doped with minor amounts of elements like Ag [3], Fe [4], Bi [5–8] and As [7, 9], has been extensively studied as an electrocatalytic material for oxygen transfer reactions.

Mixed oxides obtained directly by electrodeposition are uncommon. One instance is $Pb_8Tl_5O_{24}$ which has been obtained by anodic oxidation of a Pb^{2+} + Tl^{+} alkaline solution at room temperature [10] and used as an anode for oxygen evolution and oxidation of organics [11]. Deposition of ternary Pb–Tl–O compounds with modulation of stoichiometry has been investigated with the aim of producing ceramic superlattices [12–16].

To the best of our knowledge, no attempt has been reported to prepare mixed Pb + Mn oxides by anodic electrodeposition, although some mixed oxides like $Pb_3Mn_7O_{15}$ are known to be stable in acid medium and may be useful as electrode materials [17]. Therefore, we have undertaken a study of the anodic codeposition of PbO_2 and MnO_2, in order to assess whether mixed oxides are formed either at room temperature or after thermal annealing.

2. Experimental details

The conditions selected for the electrodeposition were similar to those described by Preisler [18] as appropriate for deposition of MnO_2. Stationary Ti plates (10 mm × 10 mm) were used as the working electrode except in the chronopotentiometric experiments in which a Ti rotating disc electrode was used. A Pt wire and a saturated calomel electrode (SCE) were used as the counter and reference electrode, respectively; accordingly, potentials are referred to the SCE.

The Ti substrate was etched in concentrated HF, then rinsed with distilled water and acetone. The electrolyte was a solution consisting of 0.7 M CH_3COOH, $Mn(CH_3COO)_2$ and $Pb(CH_3COO)_2$ in varying concentrations for a total of 0.18 M, pH adjusted to 4. Solutions were stirred in contact with the atmosphere and their temperature was maintained constant at values between 30 °C and 85 °C. Electrodeposition was carried out at constant current density and deposits were grown to about 100 μm, washed with distilled water and dried at room temperature.

All samples were annealed in air at various temperatures (500–800 °C) for 2 h. The as-deposited and annealed films were examined by scanning electron microscopy using a Philips XL 40 LaB_6 apparatus. Quantitative standardless microanalyses (EDX) were obtained using a PV 99 X-ray spectrometer equipped with an ultrathin Be window. ZAF corrections (taking into account the factors of atomic number Z, absorption A and fluorescence correction F) were made to quantitative measurements, taken with an accelerating voltage of 25 keV. The structures of the oxide films were examined by X-ray diffraction analysis using a Philips PW3710 instrument (Cu-$K\alpha$ radiation, 40 kV and 30 mA, narrow divergence slit of 1/6 degree).

3. Results and discussion

3.1. *Chronopotentiometric experiments*

Figure 1 reports some typical experiments performed at the rotating Ti disc electrode, at 85 °C, in solutions containing either (a) 0.18 M $Mn(CH_3COO)_2$ + 0.7 M CH_3COOH or (b) 0.05 M $Mn(CH_3COO)_2$ + 0.13 M $Pb(CH_3COO)_2$ + 0.7 M CH_3COOH.

On the basis of standard redox potentials [19], anodic deposition of MnO_2 should be easier than deposition of PbO_2:

$$Mn^{2+} + 2\,H_2O = MnO_2 + 4\,H^{+} + 2\,e^{-}.$$
$$E^{\circ} = 1.228 - 0.1182\,pH - \log[Mn^{2+}]\ V\ vs\ NHE. \quad (1)$$

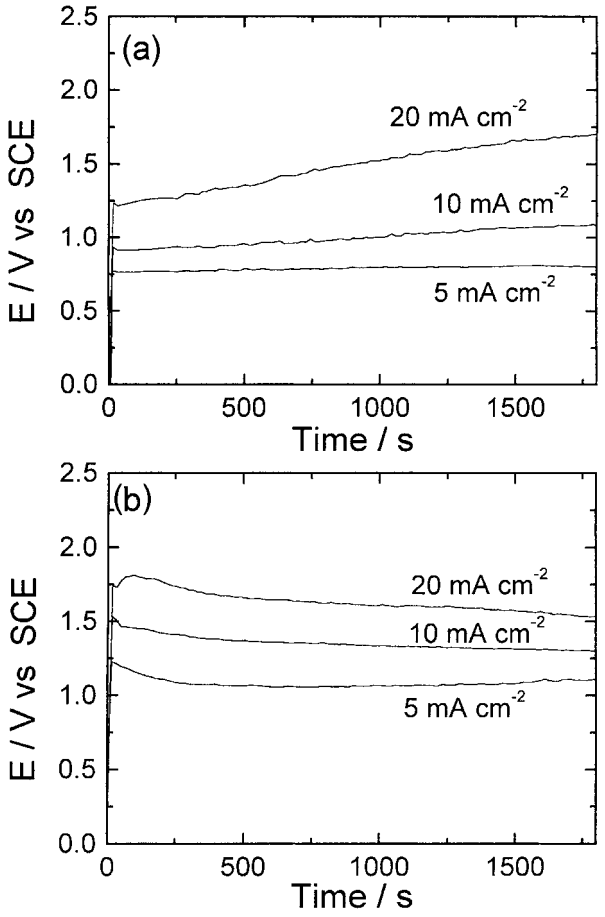

Fig. 1. Chronopotentiometric curves obtained on titanium rotating disc electrode (Ω = 2025 rpm) at various current densities. Electrolytes: (a) 0.18 M $Mn(CH_3COO)_2$ + 0.7 M CH_3COOH and (b) 0.05 M $Mn(CH_3COO)_2$ + 0.13 M $Pb(CH_3COO)_2$ + 0.7 M CH_3COOH. $T = 80$ °C.

$$Pb^{2+} + 2\,H_2O = PbO_2 + 4\,H^+ + 2\,e^-.$$
$$E^\circ = 1.449 - 0.1182\,pH - \log[Pb^{2+}]\ V\ vs\ NHE. \quad (2)$$

At pH 4 and an ionic concentration of 0.18 M equilibrium potentials would be 0.532 and 0.753 V vs SCE, respectively. Indeed, lower potentials are required for deposition of pure MnO_2 (Figure 1(a)) than for the mixed oxide (Figure 1(b)). The difference is more marked than would be expected on the basis of the reduced Mn^{2+} concentration in the latter case: the presence of Pb^{2+} and/or the formation of PbO_2 increases the overpotential for MnO_2 deposition.

In Figure 1(a) (deposition of pure MnO_2) the potential, after an initial sharp rise, remains quite stable for the lower current density, 5 mA cm^{-2}, and shows either a limited or a marked drift towards positive values at 10 and 20 mA cm^{-2}, respectively. The latter phenomenon may be attributed to the buildup of resistance either in the film bulk (MnO_2 is a poor conductor) or at the boundary between substrate and MnO_2 phase, due to the possible formation of a thin TiO_2 film of high resistivity. No such passivation phenomenon is observed during deposition of $MnO_2 + PbO_2$ (Figure 1(b)). Rather, the potential passes through a maximum at early times, due to nucleation difficulties, and then decreases more or less steadily as the film grows thicker, possibly indicating an increase of the effective electrode area. Apparently, no significant resistance is introduced during growth of the MnO_2 + PbO_2 layer.

3.2. *Effect of deposition parameters*

Figure 2 shows the effect of some important deposition parameters on the molar fraction Mn/(Mn + Pb) of the deposit, as estimated by EDX.

Figure 2(a) shows the dependence on the $Mn^{2+}/(Mn^{2+} + Pb^{2+})$ fraction in solution. It can be seen that the composition of the as-grown layers is always enriched in MnO_2 as compared to molar fractions in solution. Whereas the enrichment in the content of less 'noble' species is expected, not so obvious is the limited sensitivity to solution composition. Figure 2(b) shows the effect of current density on composition of deposited film. The Mn/(Mn + Pb) atomic ratios are higher for oxide films prepared at low current densities, and slightly decrease as the current density increases. These results are consistent with expectations for the general case of alloy deposition [20]: higher currents favour deposition of the species requiring higher overpotentials, in this case lead oxide. However, film composition appears little sensitive even to this deposition parameter. Figure 2(c) shows the dependence of film composition on temperature of the electrolytic bath. It can be seen that the Mn/(Mn + Pb) ratio depends markedly on the solution temperature below 50 °C: almost pure PbO_2 was deposited at 30 °C. The Mn content increases rapidly on increasing the temperature to 50 °C, then changes very little upon further increases.

Figures 2(a)–(c) show that, in a wide range of experimental conditions, the relative amounts of Mn and Pb in the deposit approach those of the known mixed oxide $Pb_3Mn_7O_{15}$. One can therefore speculate that deposition of the two metal oxides is not completely independent, but a strong interaction between them tends to determine the deposit composition. The electrodeposition of well-defined compounds has been often observed in the case of semiconducting transition metal chalcogenides [21–24]. In the present case of Mn + Pb oxides, the experimental evidence collected so far is not sufficient to elaborate on the mechanism of formation of a stoichiometric compound.

The effect of temperature on current efficiencies was monitored. The percentage current efficiencies $\eta(\%)$ were estimated from deposit weight and composition, assuming formation of oxides with stoichiometry MO_2 (M = Pb, Mn), according to the formula:

$$\eta = \frac{2F}{Q} \times \frac{W}{x_{Mn} w_{MnO_2} + x_{Pb} w_{PbO_2}} \times 100 \quad (3)$$

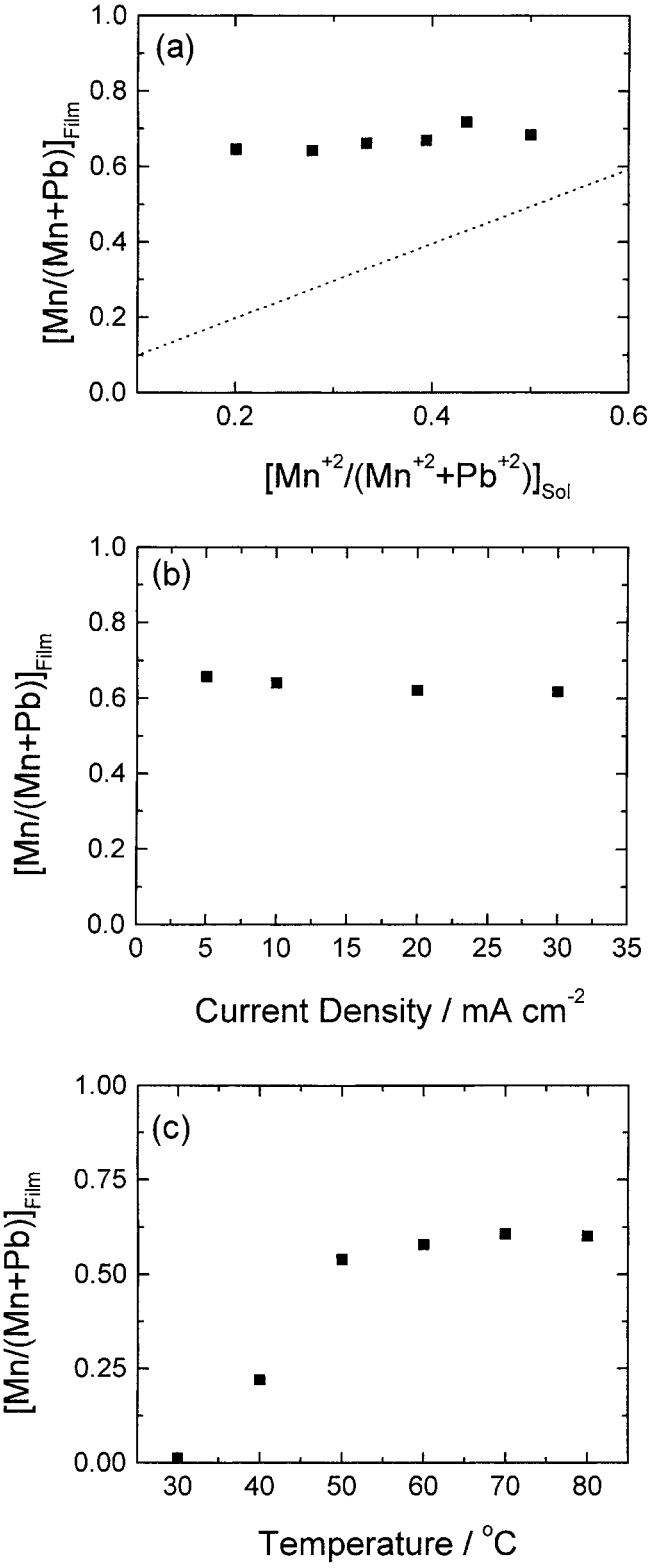

Fig. 2. Atomic ratio Mn/(Mn + Pb) in the as-grown film as a function of (a) the Mn/(Mn + Pb) ratio in solution. Current density 10 mA cm^{-2}, $T = 80\,°C$; (b) current density. Bath: 0.05 M $Mn(CH_3COO)_2$ + 0.13 M $Pb(CH_3COO)_2$ + 0.7 M CH_3COOH; $T = 80\,°C$; (c) bath temperature. Same bath of Figure 2(b), current density 10 mA cm^{-2}.

where W is the electrodeposited mass; F is the faradaic constant; 2 is the number of electrons necessary to deposit a molecule of MO_2; Q is the transferred charge; x is the atomic fraction of the given element and w the molecular mass of the relevant oxide. The observed dependence shows (Figure 3) a gradual increase from a few percent at 30 °C to about 80% at 80 °C.

During low temperature electrolyses, characterized by a low η percentage and a high Pb content in the deposit, formation of a brown colloidal suspension occurs in the electrolyte. These facts may be interpreted within the scheme of MnO_2 formation [18]:

$$2\,Mn^{2+} \longrightarrow 2\,Mn^{3+} + 2\,e^- \quad (4a)$$

$$2\,Mn^{3+} \longrightarrow Mn^{2+} + Mn^{4+} \quad (4b)$$

$$Mn^{4+} + 2\,H_2O \longrightarrow MnO_2 + 4\,H^+ \quad (4c)$$

assuming that low temperatures may slow down the disproportionation process of Reaction 4(b). If this is the case, a larger fraction of the Mn(III) ions will live long enough to back diffuse into bulk solution where the process will be completed by Reaction 4(c). The loss of MnO_2 would account for the observed lower current yield and higher Pb content.

3.3. *Characterization of as deposited and annealed films*

The electrodeposited oxide layers were analysed by X-ray diffraction. All samples directly obtained by electrodeposition showed peaks due to either MnO_2 or PbO_2, whatever their Mn/Pb ratio. No evidence of the formation of crystalline $Pb_3Mn_7O_{15}$ was provided by the same spectra. Thus, there is an apparent contradiction between the composition data of Figure 2, suggesting a tendency to form a deposit of composition close to $Pb_3Mn_7O_{15}$, and the XRD results. However, this discrepancy may be reconciled if we assume that the as-grown deposits largely consist of amorphous $Pb_3Mn_7O_{15}$, but the XRD pattern is dominated by crystalline PbO_2 and MnO_2.

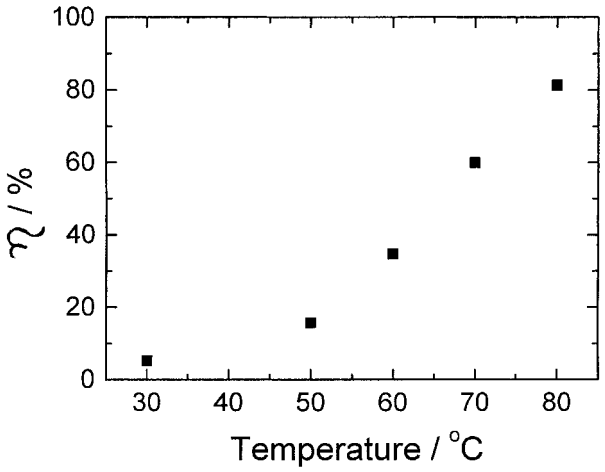

Fig. 3. Percentage current efficiency, η, of the electrodeposition process (estimated from Equation 3) as a function of bath temperature.

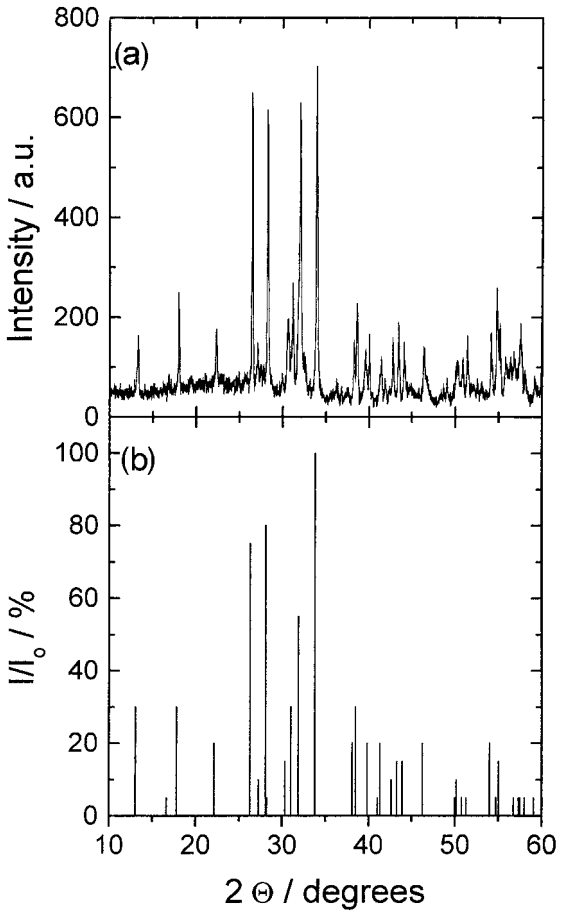

Fig. 4. (a) X-ray diffraction pattern of the oxide mixture after annealing at 800 °C compared with (b) JCPDS pattern of the $Pb_3Mn_7O_{15}$ compound [25].

Samples were then annealed in the air (at 800 °C, typically for 2 h) and examined again in order to detect the presence of mixed oxides. Figure 4 shows an X-ray diffractogram of an annealed sample, compared with the spectrum reported in the JCPDS cards for $Pb_3Mn_7O_{15}$ [25]. The good matching and the absence of peaks typical of MnO_2 and PbO_2 are clear indications that crystalline $Pb_3Mn_7O_{15}$ has formed from reaction of simple binary oxides. Crystallization of amorphous $Pb_3Mn_7O_{15}$ is probably an additional effect of heating.

It is interesting to note that electrodeposits with a Mn/Pb ratio close to 2.33 (corresponding to the $Pb_3Mn_7O_{15}$ stoichiometry) maintained this ratio almost unchanged upon annealing, while the Mn/Pb ratio of deposits initially Pb-rich (Mn/Pb as low as 1.5) shifted towards the stoichiometric value. XRD spectra similar to that shown in Figure 4 were obtained in both cases. Thus, it can be concluded that during annealing both oxygen and PbO were lost. The latter process is of minor importance for stoichiometric deposits, possibly because the formation of the mixed oxide prevents PbO evaporation.

4. Conclusions

Simultaneous oxidation of Mn^{2+} and Pb^{2+} ions in an acetate bath yields deposits consisting of crystalline MnO_2 and PbO_2 and probably a ternary amorphous phase. Deposits with a ratio Pb/Mn = 3/7 were easily obtained at $T > 50$ °C, but no formation of crystalline $Pb_3Mn_7O_{15}$ or other mixed oxides was detected in the as-deposited material. Oxide mixtures could be quantitatively converted to $Pb_3Mn_7O_{15}$ by annealing at 800 °C.

Acknowledgements

The authors gratefully acknowledge financial support by CNR-Progetto Finalizzato Materiali Speciali per Tecnologie Avanzate II. One of us (E.A.D.) carried out this work with the support of the ICTP Programme for Research and Training in Italian Laboratories, Trieste, Italy, which is kindly acknowledged.

References

1. F. Beck, *in* A.T. Kuhn (Ed), 'The Electrochemistry of Lead' (Academic Press, London, 1979), Chapter 4.
2. S. Trasatti (Ed), 'Electrodes of Conductive Metallic Oxides', Parts A and B (Elsevier Scientific, New York, 1980).
3. J. Ge and D.C. Johnson, *J. Electrochem. Soc.* **142** (1995) 1525.
4. J. Feng and D.C. Johnson, *J. Electrochem. Soc.* **137** (1990) 507.
5. I.H. Yeo, S. Kim, R. Jacobson and D.C. Johnson, *J. Electrochem. Soc.* **136** (1989) 1395.
6. W.R. LaCourse, Y.L. Hsiao and D.C. Johnson, *J. Electrochem. Soc.* **136** (1989) 3714.
7. H. Chang and D.C. Johnson, *J. Electrochem. Soc.* **137** (1990) 2452.
8. K.T. Kawagoe and D.C. Johnson, *J. Electrochem. Soc.* **141** (1994) 507.
9. I.H. Yeo, Y.S. Lee and D.C. Johnson, *Electrochim. Acta* **37** (1992) 1811.
10. M. Sakai, T. Sekine and Y. Yamazaki, *J. Electrochem. Soc.* **130** (1983) 1631.
11. W. Tillmetz and D. Wabner, *Z. Naturforsch.* **39b** (1984) 594.
12. J.A. Switzer, M.J. Shane and R.J. Phillips, *Science* **247** (1990) 444.
13. J.A. Switzer, R.P. Raffaele, R.J. Phillips, C.J. Hung and T.D. Golden, *Science*, **258** (1992) 1918.
14. T.D. Golden, R.P. Raffaele and A.J. Switzer, *Appl. Phys. Lett.* **63** (1993) 1501.
15. J.A. Switzer and T.D. Golden, *Adv. Mater.* **5** (1993) 474.
16. J.A. Switzer, C.J. Hung, B.E. Breyfogle, M.G. Shumsky, R. Van Leeuwen and T.D. Golden, *Science* **264** (1994) 1573.
17. B. Latourrette, M. Devalette, F. Guillen and C. Fouassier, *Mat. Res. Bull.* **13** (1978) 567.
18. E. Preisler, *J. Appl. Electrochem.* **6** (1976) 301.
19. M. Pourbaix, 'Atlas d'Equilibres Electrochimiques' (Gauthier-Villars, Paris, 1963).
20. A. Brenner, 'Electrodeposition of Alloys' (Academic Press, New York, 1963).
21. G. Hodes, J. Manassen and D. Cahen, *Nature* **261** (1976) 601.
22. M. Tomkiewicz, I. Ling and W.S. Parsons, *J. Electrochem. Soc.* **129** (1982) 2016.
23. E. Mori and K. Rajeshwar, *J. Electroanal. Chem.* **258** (1988) 415.
24. C.D. Lokhande, *J. Electrochem. Soc.* **134** (1987) 1727.
25. *JCPDS Card* 36-840 (1996).